SEÇÃO V - GÊNESE, MORFOLOGIA E CLASSIFICAÇÃO DO SOLO

SOIL STRUCTURE TRANSFORMATIONS FROM FERRALIC TO NITIC HORIZONS ON A TOPOSEQUENCE IN SOUTHEASTERN BRAZIL[1]

Miguel Cooper[2], Pablo Vidal-Torrado[3] & Michel Grimaldi[4]

ABSTRACT

The soil structure transformation from ferralic to nitic horizons was studied in a toposequence on quaternary red clayey sediments and diabase in Piracicaba (SP), Brazil. Morphological and micromorphological studies, image analysis, soil water characteristic curves and monitoring of (total) soil water potential head were used. The presence of polyconcave vughs, clayskins and planar voids shows that the vertical and lateral transition and structural transformation from ferralic to nitic horizons is given by the coalescence of the microaggregates, probably due to tensions created in a drier period in the past. Changes to a more humid climate with a defined dry season and alternate drying and wetting cycles resulted in the fissuration of the previously coalesced material, forming polyhedral aggregates and microaggregates. Simultaneously, clay illuviation filled the voids and together with the compacting action of the biological activity of these soils contributed to the coalescence of microaggregates.

Index terms: Ferralsols, Nitisols, soil micromorphology, image analysis, soil water dynamics.

RESUMO: *TRANSFORMAÇÕES DA ESTRUTURA ENTRE HORIZONTES B LATOSSÓLICO E B NÍTICO EM UMA TOPOSSEQUÊNCIA NO SUDESTE DO BRASIL*

A transformação estrutural entre horizontes B latossólico e B nítico foi estudada numa topossequência sobre sedimentos vermelhos quaternários e diabásio em Piracicaba (SP). Estudos morfológicos e micromorfológicos, análises de imagem, curvas de retenção e o monitoramento do potencial total da água no solo foram utilizados. A presença de cavidades

[1] Study funded by FAPESP. Received for publication in August 2009 and approved in July 2010.

[2] Associate Professor of Departamento de Ciência do Solo da ESALQ/USP. Caixa Postal 09, CEP 13418-900 Piracicaba (SP), Brasil. CNPq fellow. E-mail: mcooper@esalq.usp.br

[3] Full Professor of Departamento de Ciência do Solo da ESALQ/USP. Caixa Postal 09, CEP 13418-900 Piracicaba (SP), Brasil. E-mail: pablo@esalq.usp.br. CNPq fellow.

[4] Researcher of IRD/France, 32 avenue Henri Varagnat 93143 Bondy Cedex, France. E-mail: Michel.Grimaldi@ird.fr

policôncavas, revestimentos de argila e poros fissurais mostrou que a transição vertical e lateral e a transformação estrutural entre os horizontes B latossólico e B nítico ocorrem pela coalescência da estrutura microgranular, devido provavelmente a tensões criadas durante um período mais seco que o atual. A mudança para climas mais úmidos com estação seca bem definida favoreceu a instalação de ciclos de umedecimento e secagem mais frequentes, que resultaram na fissuração do material previamente coalescido, formando agregados e microagregados poliédricos. Ao mesmo tempo em que esses processos estavam acontecendo, a iluviação de argila preenchia o espaço poroso e, junto com a ação de compactação provocada pela atividade biológica, auxiliava na coalescência dos microagregados.

Termos de indexação: Latossolo, Nitossolo, micromorfologia do solo, análise de imagens, dinâmica da água no solo.

INTRODUCTION

Soil surveys and the understanding of processes within soil systems are facilitated by the knowledge on spatial soil distribution in the landscape and the interrelations between horizons of the different soils. In tropical regions where basalt or diabase dominate as parent materials, it is common to find extremely deep and highly weathered soils with little differentiation between horizons on flat summits (Ferralsols). At the transition from flat to sloping surfaces these homogeneous soils evolve to soils that are characterized by the presence of a subangular blocky structure in the upper part of B horizons (nitic horizon) and micro-granular structure (ferralic horizon) in the deeper part of B horizons. On steeper slopes the blocky-structure horizon is thicker while the other micro-granular horizon is thinner until its total disappearance, leading to the formation of the blocky structure horizons along the soil profile (Nitisols).

The continuous debate of the last three decades has given rise to a series of hypotheses on the structural transformation from ferralic to argic or nitic horizons in tropical soil genesis (Lepsch & Buol, 1975; Lepsch et al., 1977; Moniz & Buol, 1982; Birkeland, 1984; Bullock & Thompson, 1985; Fedoroff & Eswaran, 1985; Miklós, 1992; Vidal-Torrado & Lepsch, 1993; Vidal-Torrado et al., 1999). These hypotheses vary from the filling of the porosity by illuvial clays deposited in the packing voids between the micro-granular aggregates, to the coalescence of the micro-granular structure by alternate drying and wetting cycles, either under the present humid or under drier climatic conditions in the past. According to Moniz & Buol (1982), Miklós (1992) and Vidal-Torrado et al. (1999) the coalescence of microaggregates that transforms a micro-granular structure into a subangular blocky structure is due to an interaction between soil structure and its hydrodynamic behavior.

Most studies cited above are based on qualitative morphological, rather than on quantitative morphological and physical data. Using qualitative and quantitative methods to determine the soil structure organization and soil water dynamics, the purpose of this study was a deeper understanding of the processes of structural transformation from ferralic horizons with a micro-granular structure to nitic horizons with a subangular blocky structure, developed on a toposequence over diabase.

MATERIALS AND METHODS

The study site is located in Piracicaba, São Paulo State, Brazil (22 ° 42 ' 30 " S, 47 ° 38 ' 00 " W), at an elevation of about 546 m asl. The mean annual rainfall is 1,277 mm with a dry period from April to September, mean monthly rainfall of 43 mm and mean annual temperature of 21.5 ºC. January is the hottest month (mean 24.4 ºC) and July the coldest (mean 17.4 ºC). The study was conducted on the summit and shoulder segments of a toposequence underlain by a Cenozoic red clayey deposit and diabase (Cooper et al., 2002).

Soil morphology was described in three pits along the toposequence according to Lemos & Santos (1996) and soils were classified according to the World Reference Base (ISSS-ISRIC-FAO, 1998). The geometrical distribution of the soil horizons in the toposequence was detected by the method developed by Boulet et al. (1982).

Large thin sections (9 x 16 cm) of resin-impregnated blocks were prepared for micromorphological observations. Undisturbed and oriented samples were impregnated with non-saturated polyester resin (Crystic SR 17449) diluted with acetone plus a fluorescent dye to enable pore distinction under UV light (Murphy, 1986). Smaller thin sections (3 x 4.5 cm) were also prepared for examination under a scanning electron microscope (SEM, Philips XL20). These samples were polished with diamond grains of decreasing size and carbon-coated for observation under SEM in backscattered electron mode. Soil micromorphological descriptions followed the criteria described by Bullock et al. (1985) and some terms of textural pedofeatures were used as proposed by Brewer (1976).

Digital images of the large thin sections were taken with a monochromatic CCD camera (resolution of 768 x 576 pixels in a 100 mm^2 pixel area). The SEM images had a resolution of 712 x 484 pixels with a pixel area of 1 mm^2. Images were processed on a SUN Spark IPC system using Noesis Visilog image analysis software. Total porosity (tpa) was calculated as the sum of the areas of all pores or *poroids* (concept defined by Moran et al., 1988, adopted here) divided by the total field area, in percentage. The *poroids* were divided into three shape groups, i.e. rounded, elongated and irregular. Two indexes were used to determine the poroid shape:

$$I_1 = \frac{P^2}{(4\pi A)} \quad (1)$$

where P is the perimeter of the poroid and A its area, and

$$I_2 = \frac{\frac{1}{m}\sum_i (N_I)_i}{\frac{1}{n}\sum_j (D_F)_j} \quad (2)$$

where N_I is the number of intercepts of an object in direction i (i = 0°, 45°, 90°, and 135°), D_F is the Feret diameter of an object in direction j (j = 0° and 90°), m is number of i directions and n is the number of j directions. This index is used as a complement to index I_1 for a higher precision in the separation of the shape groups. The criteria for the distinction between shape groups and their sizes are shown in tables 1 and 2.

Soil-moisture retention curves were determined using a tension plate for the matric suction values below 100 hPa and a pressure membrane apparatus for matric suctions above 100 hPa. The matric suctions used for the determination of the soil-moisture retention curves were 0, 5, 10, 30, 50, 80, 100, 330, 1,000, 5,000 and 15,000 hPa.

Variations of the (total) soil water potential head between the tropical wet (spring-summer) and dry seasons (autumn-winter) were monitored from October 1997 to June 1998. Mercury manometer tensiometers were installed at four locations along the transect to monitor the daily total water potential head from October 1997 (end of dry season) to June 1998 (peak of dry season). The tensiometers were distributed in four sets of seven on the summit and shoulder of the toposequence. In each set, the tensiometers were installed at depths of 0.1, 0.3, 0.6, 0.8, 1.0, 1.2, and 1.5 m determined according to the geometrical distribution of the horizons on the toposequence. Total soil water potential head was accurately measured in the range 0 to -750 hPa. The total water potential head was also monitored during specific rain events. Tensile strength was measured before the storm, during the storm at 15' intervals and after the storm at 2 h intervals during 24 h.

Table 1. Definition of the shape classes of the poroids

Poroid	Shape index	
	I_1	I_2
Rounded (Roun)	$I_1 \leq 5$	
Elongated (Elon)	$5 < I_1 \leq 25$	$\leq 2{,}2$
Irregular (Irr)	$5 < I_1 \leq 25$ ou > 25	$> 2{,}2$

Table 2. Definition of the size and shape classes of the poroids

Size class	Shape class		
	Rounded	Elongated	Irregular
mm^2			
0,001– 0,01	$Roun_s$	$Elon_s$	Irr_s
0,01 – 0,1	$Roun_m$	$Elon_m$	Irr_m
> 0,1	$Roun_l$	$Elon_l$	Irr_l

s: small; m: medium; l: large.

RESULTS

Soil morphology and distribution

The location of the three pedons, the lateral distribution of the horizons and the slope segments are shown in figure 1. The soils were classified as Ferralic Nitisols for pits 1 and 2 (T1 and T2) and Rhodic Nitisol for pit 3 (T3) according to the World Reference Base (ISSS-ISRIC-FAO, 1998). Morphological descriptions (Lemos & Santos, 1996) of the soil profiles are shown in table 3. The morphological descriptions and geometry of the horizons show the presence of ferralic and nitic horizons. Figure 1 shows well-developed nitic horizons in all segments of the transect. The thickness of the Bni1 and Bni2 horizons is steady along the toposequence, unlike the Bfl1 and Bfl2 horizons, which thin out from the upper shoulder to the lower shoulder segments or even eventually disappear.

The ferralic horizons are very porous with a micro-granular structure and clayey texture (Table 3). The nitic horizons have a well-developed subangular blocky structure with fissures separating the aggregates and also have a clayey texture. The macromorphological observation did not evidence a better developed subangular blocky structure between Bni1 or Bni2 and Bni3, Bni4 and Bni5 (Table 3). No textural gradient was found in the studied soil profiles along the transect. Biological activity is important in both nitic and ferralic horizons and was evidenced by vughs and channels with or without fillings. Along the descending toposequence, one of the most striking features is the progressive lateral and vertical

structural transition (Figure 1). This transition results in the gradual thickening of the nitic horizon and a thinning of the ferralic horizon, until the total disappearance of the ferralic horizon on the shoulder segment.

Soil micromorphology

Important aspects of the structural evolution from ferralic to nitic horizons were revealed in the micromorphological descriptions (summarized in

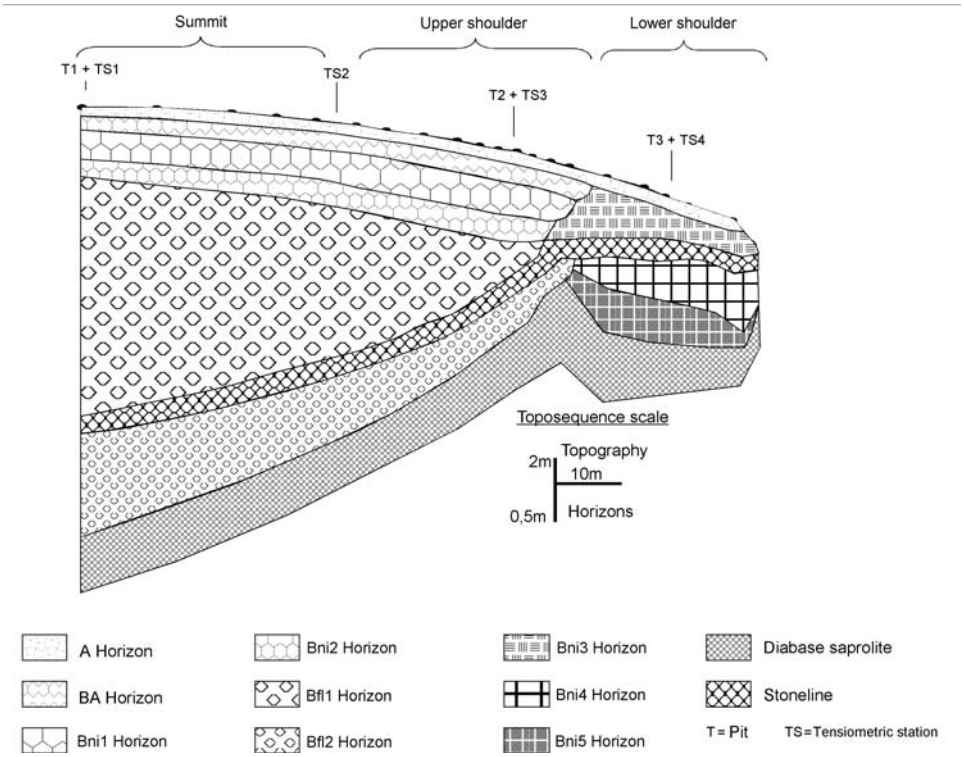

Figure 1. Soil distribution on the toposequence (Bni: nitic horizon; Bfl: ferralic horizon).

Table 3. Field morphology descriptions

Horizon	Depth	Structure[1]	Colour	Texture	Clay coating [2]	Consistence[3]
	cm		Profile 1: Ferralic Nitisol			
A	0 - 10	2; m; sb	2,5YR 3/3	clayey	-	h; fr
BA	10 - 30	3; m; sb	2,5YR 3/6	clayey	-	h; fr
Bni1	30 - 70	3; m; sb	2,5YR 3/4	clayey	co; w	h; fr
Bni2	70 - 90	3, m; sb	2,5YR 3/4	clayey	f; w	h; fr
Bfl	90 - 200+	1; m; sb + gr	2,5YR 3/4	clayey	-	h; vfr
			Profile 2: Ferralic Nitisol			
A	0 - 16	3; f; gr; sb	2,5YR 3/4	clayey	-	h; fr
BA	16 - 34	3; m; sb	2,5YR 3/6	clayey		h; fr
Bni1	34 - 77	3; m; sb	2,5YR 3/6	clayey	ab; st	h; fr
Bni2	77 - 103	2; m; sb; gr	2,5YR3/6	clayey	c; m	h; fr
Bfl1	103 - 130	3; f; gr	2,5YR 3/6	clayey	-	vfr
Stoneline	130 - 142	-	-	-	-	-
Bfl2	142 - 179	3; f; gr;	2,5YR 3/6	clayey	-	vfr
			Profile 3: Rhodic Nitisol			
A	0 - 15	2; m; sb	2,5 2,75/4	clayey	-	h; fr
Bni3	15 - 35	3; m; sb + pr	2,5 2,75/4	clayey	ab; m	h; fr
Stoneline	35 - 50	-	-	-	-	-
Bni4	50 - 100	3; m; sb	2,5 3/6	clayey	ab; m	h; fr
Bni5	100 - 150	2; m; sb	2,5 3,5/6	clayey	ab; m	h; fr

[1] 3: strong; 2: moderate; 1: weak; f: fine; m: medium; gr: granular; sb: subangular blocky; pr: prismatic. [2] f: few; c: common; ab: abundant; w: weak; m: moderate; st: strong. [3] (dry) h: hard; (humid) fr: friable; vfr: very friable.

table 4). The micromorphology of the nitic and ferralic horizons of the three profiles showed a vertical and lateral compaction process evidenced by a gradual coalescence of the micro-granular structure of the ferralic horizons (Bfl). Gradual changes in the C/F (coarse/fine particles)-related distributions between and within the Bfl horizons and Bni horizons together with changes in the void morphology and consequently in soil structure, are clear evidence of this vertical and lateral compaction process (Figure 2).

Along the ascending soil profiles, the C/F related distribution gradually changes from enaulic in the Bfl horizons to a porphyric enaulic intermediate stage in the Bni2 transition horizons and to an open porphyric in the Bni1 horizons. Correlated with the changes in the C/F related distribution, the soil structure gradually changes from micro-granular with some coalesced micro-granular zones in the Bfl horizons to a coalesced micro-granular structure in the Bni2 transition horizons, and to a blocky structure with coalesced micro-granular zones in the Bn1 horizons. This structure transformation ("variation" or "evolution") in the soil profiles affects the soil voids, which, in the same sense, evolve from packing voids in the Bfl horizons to polyconcave vughs and packing voids in the transition horizons, and to polyconcave vughs and planes in the Bni1 horizons (Table 4, Figure 2).

Along the toposequence, the C/F related distribution of the Bfl horizons on the summit is enaulic and evolves to porphyric-enaulic on the upper shoulder and to open porphyric at the end of the shoulder (Bni5 horizon). The Bni horizons that have a porphyric C/F related distribution with some locally enaulic zones on the summit, evolve to open porphyric in the upper shoulder and lower shoulder segments.

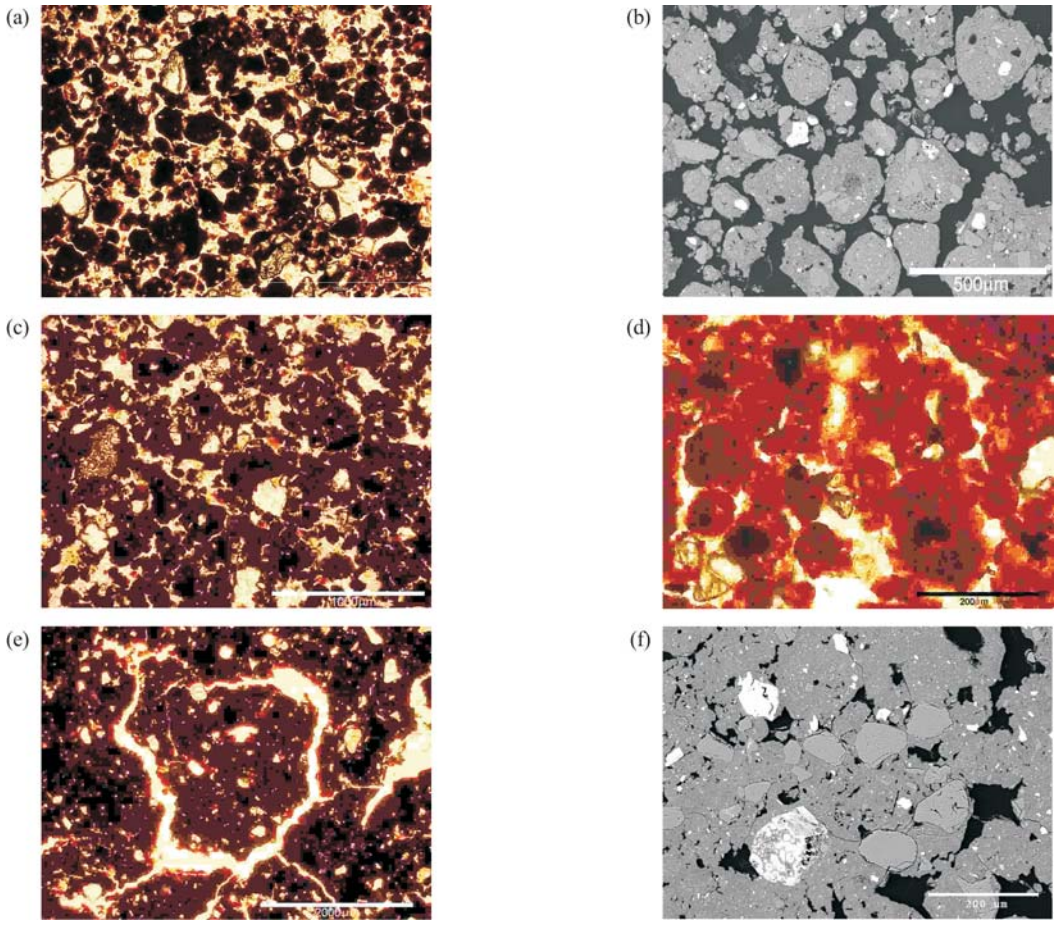

Figure 2. Microphotographs of the transformation process between the Bfl (profile 1) and the Bni (profile 1) horizons. (a) Micro-granular structure with packing voids and an enaulic C/F related distribution, (b) Backscattered electron image detailing the micro-granular structure, (c) Coalesced micro-granular aggregates in the transition horizons (Bni2, profile 1), (d) Detail of the coalesced micro-granular aggregates and the formation of polyconcave vughs (indicated as PV), (e) Porphyric polyhedral aggregates separated by planes and polyconcave vughs in the interior of the aggregates, (f) Detail of the polyconcave vughs (in black) in the interior of the polyhedral aggregates (backscattered electron image).

Table 4. Micromorphological characteristics of the nitic and ferralic horizons

Horizon	Depth	C/F related distribution	Microstructure	Void	Pedofeature
	cm		Profile 1: Ferralic Nitisol		
Bni1	30-70	Open porphyric, locally enaulic	Subangular blocky with coalesced micro-granular structure (dominant), micro-granular structure	Policoncave vughs (dominant), biological vughs, planes, packing voids	Clay coatings (ferri-argillans)
Bni2	70-90	Enaulic (dominant), open porphyric	Micro-granular with coalesced micro-granular structure (dominant), subangular blocky structure	Packing voids, policoncave vughs, planes, biological vughs	Clay coatings (ferri-argillans)
Bfl	90-200+	Enaulic	Micro-granular (dominant), coalesced micro-granular structure	Packing voids (dominant), policoncave vughs, channels, biological vughs	Loose continuous infillings in channels and biological vughs
			Profile 2: Ferralic Nitisol		
Bni1	34-77	Open porphyric	Subangular blocky structure (dominant), micro-granular	Planes (dominant), policoncave vughs, packing voids, channels, vughs	Clay coatings (ferri-argillans)
Bni2	77-103	Porphyric-enaulic (dominant), enaulic	Subangular blocky structure (dominant), coalesced micro-granular structure	Policoncave vughs (dominant), planes, vughs, channels	Clay coatings (ferri-argilans), loose continuous infillings in channels and vughs
Bfl1	103-130	Porphyric-enaulic locally enaulic	Coalesced micro-granular structure (dominant), micro-granular, subangular blocky structure	Policoncave vughs (dominant), channels, vughs, planes	Loose continuous infillings in channels and vughs.
Bfl2	142-17	Enaulic (dominant), porphyric-enaulic	Micro-granular (dominant), coalesced micro-granular structure, subangular blocky structure	Packing voids (dominant), policoncave vughs, channels, vughs, planes	–
			Profile 3: Rhodic Nitisol		
Bni3	15-35	Open porphyric	Subangular blocky structure	Planes (dominant), policoncave vughs, biological vughs	Clay coatings (ferri-argillans), loose continuous infillings
Bni4	50-100	Open porphyric	Subangular blocky structure	Policoncave vughs (dominant), planes, biological vughs and channels	Clay coatings (ferri-argillans), loose continuous infillings
Bni5	100-150	Open porphyric (dominant), porphyric-enaulic	Subangular blocky structure (dominant), coalesced micro-granular structure	Policoncave vughs (dominant), planes, biological vughs and channels	Clay coatings (ferri-argillans), loose continuous infillings

From the summit to the shoulder segments, the soil structure and voids in the Bfl horizon evolve from a micro-granular structure with few coalesced micro-granular zones and packing voids to an intermediate stage with an increase of coalesced micro-granular features which results in similar proportions between coalesced micro-granular and micro-granular structures where polyconcave vughs and packing voids are present (Table 4, Figure 2). This intermediate stage evolves finally to a subangular blocky structure with locally coalesced micro-granular zones dominated by polyconcave vughs and planes. The lateral structure evolution in the Bni horizon shows a subangular blocky structure throughout the toposequence with the presence of coalesced micro-granular zones in the summit position that gradually disappear in the shoulder positions (Figure 2). Following the evolution of the soil structure in the Bni horizons, polyconcave vughs with few planes dominate the summit segment; this type of vughs plays a secondary role in the shoulder positions where planar voids predominate. In the Bni2 transition horizon

this lateral structure and void transformations were also observed. These transformations are characterized by the passage, from the summit to the upper and lower shoulder segments, of a micro-granular structure with coalesced micro-granular zones where packing voids and polyconcave vughs dominate, to a subangular blocky structure with coalesced micro-granular zones in which polyconcave vughs and planes are present and finally to a subangular blocky structure with polyconcave vughs and planes (Table 4, Figure 2).

In the Bni1, Bni3 and Bni4 horizons with an open porphyric C/F related distribution and in the transition Bni2 horizons with a porphyric-enaulic C/F related distribution, planar and micro-planar voids develop on the borders of the subangular blocky aggregates and in the coalesced micro-granular zones. As a consequence of the formation of these types of voids, polyhedral micro-granular aggregates are formed or previously coalesced micro-granular aggregates are individualized, characterizing an intense fissuration process in some areas of these horizons (Figure 3a,b).

Clay coatings were found in all Bni horizons of the toposequence. They are located mainly in the polyconcave vughs or in the packing voids of the coalesced micro-granular zones and in the planar voids separating the subangular blocky aggregates in these horizons (Figure 3 d). They consist of clay and Fe oxides and were classified according to Brewer (1976) as ferri-argillans. Although no textural gradient was observed in these soils, the clay coatings are quite numerous and may have been formed by a local clay redistribution due to clay dispersion processes (Cooper & Vidal-Torrado, 2005).

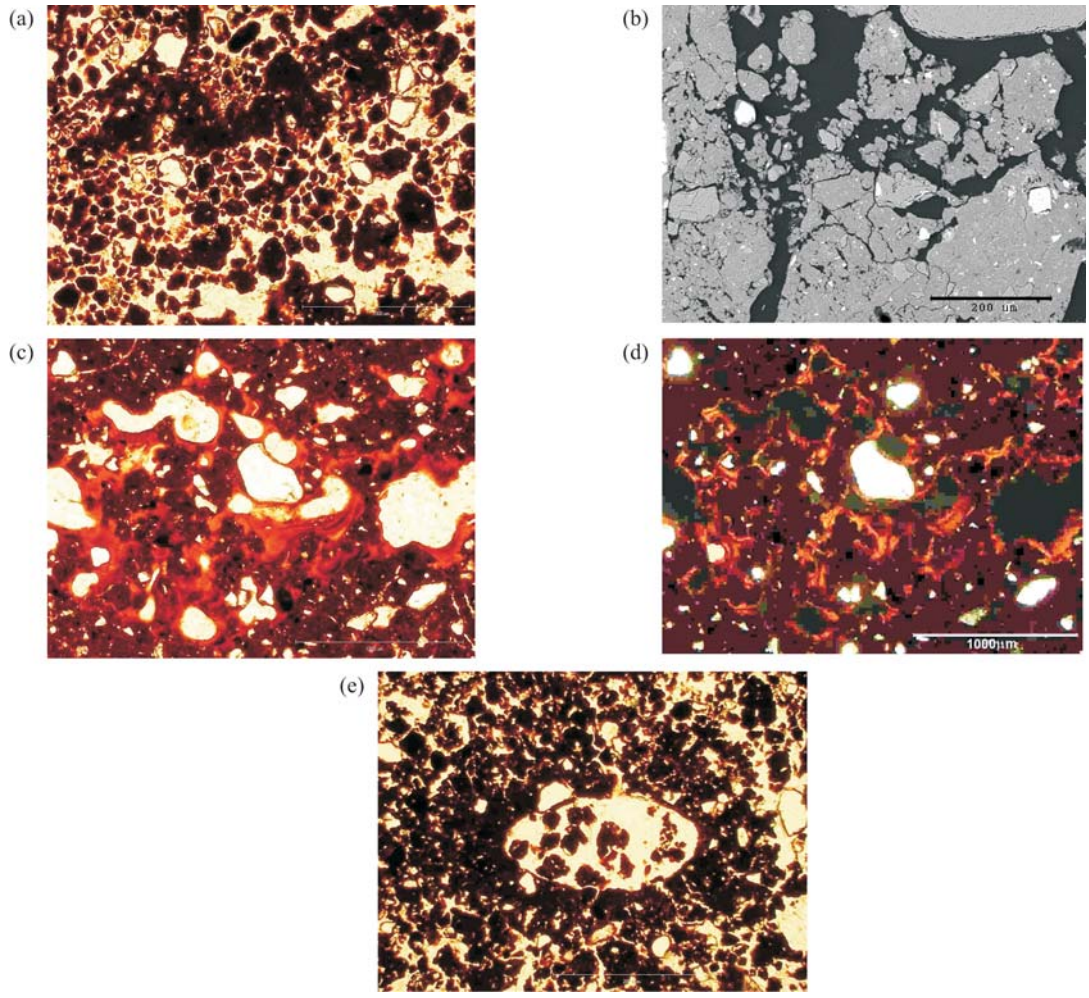

Figure 3. Microphotographs of the micro-fissuration and illuviation processes. (a) Dismantling of the porphyric C/F related distribution by fissuration processes forming micro-granular aggregates (Horizon Bn2, profile 1), (b) backscattered electron image detailing the micro-fissuration process (voids in black), (c) clay coatings filling the packing voids and polyconcave vughs cementing the micro-granular aggregates (PPL) (Horizon Bn1, profile 2), (d) same image in XPL, (e) biological vugh with loose and continuous infillings and dense walls due to compression.

The biological activity is high throughout the toposequence. Numerous biological vughs and channels are present in the soil thin sections of all horizons. Most of them have loose and continuous infillings formed mainly by rounded and polyhedral micro-granular aggregates, respectively (Figure 3e). These micro-granular aggregates could be residues of the action of the soil fauna or pedoturbation processes. An important feature in these biological vughs and channels is the compaction of the walls due to the pressure exerted by the roots or soil fauna during the opening of these voids.

Image analysis

The total area of the thin section occupied by pores (tpa) decreased vertically from the Bfl horizons to the Bni horizons in the first two pits (Figure 4). In pit T3 tpa was lowest in Bni3 and Bni4 horizons, where the blocky structure in the toposequence had developed most. The decrease in the tpa was also observed laterally within the soil horizons between T1 and T3.

In T1 and T2, a decrease in the amount of irregular voids was observed from the Bfl to the Bni horizons. The rounded voids initially increased from Bfl to the transition horizons (Bni2/Bfl in T1 and Bfl1 in T2) and later decreased in the Bni horizons of T1 and T2 (Figure 4). These changes evidence the formation of polyconcave vughs from the irregular voids and the coalescence of the micro-granular structure. The formation of the blocky structure with a dense and porphyric groundmass together with the clay illuviation in the Bni horizons, affecting size and amount of the polyconcave vughs, explain the decrease of the rounded voids. Expansion and contraction processes (due to wet and dry seasons) that can form the blocky and polyhedral micro-granular aggregates could be responsible for the presence of elongated voids.

Differing from T1 and T2, the void distribution in T3 was similar in all horizons. In these, the rounded vughs were dominant. The presence of irregular voids was mainly due to biological activity and the elongated voids represent the planes that separate the blocky aggregates that dominate in this profile.

These vertical and lateral changes in the pore shape between these horizons agree with the micromorphological observations that showed a gradual compaction process that leads to changes in the morphology of the soil structure and voids.

Soil water characteristic curves

The vertical and lateral changes in structure and porosity observed in the micromorphological descriptions and image analysis influence the behavior of the soil water characteristic curves of the different horizons of this toposequence (Figures 5 and 6).

Figure 5 illustrates the soil water characteristic curves of the Bni and Bfl horizons in the three pits. In T1, the differences observed in the gradient of the soil water characteristic curves between the Bfl and Bni horizons represent the changes in aggregation, pore size and pore morphology that occur vertically

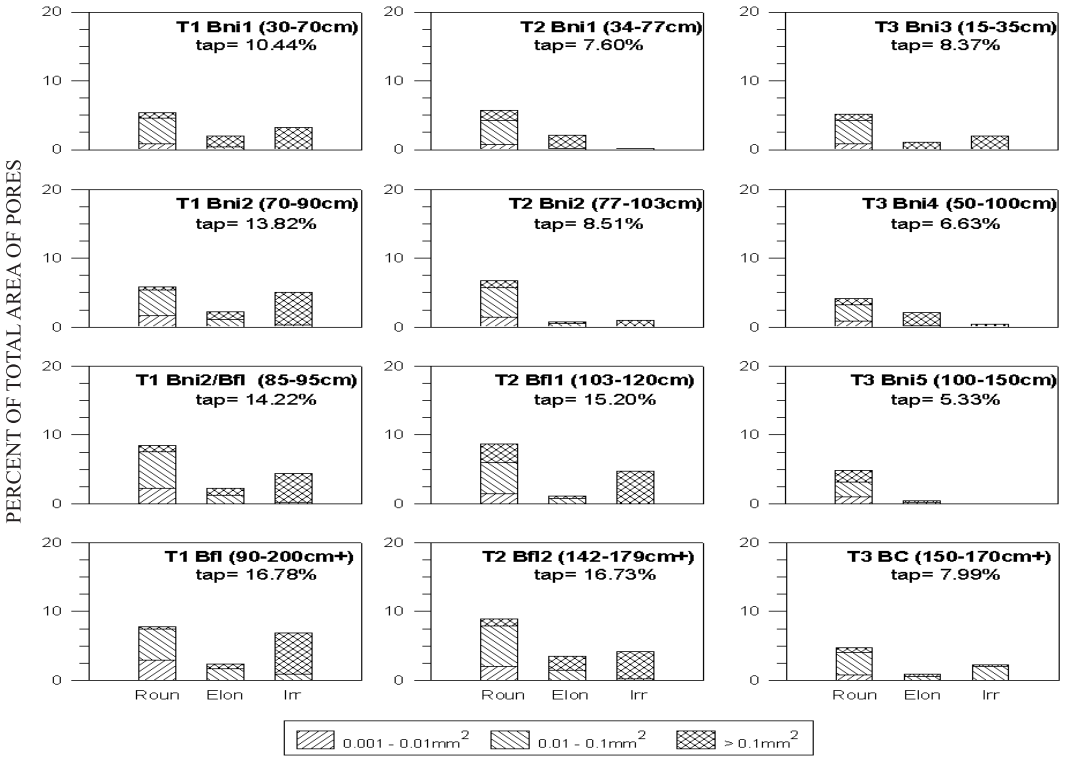

Figure 4. Pore distribution according to area and shape.

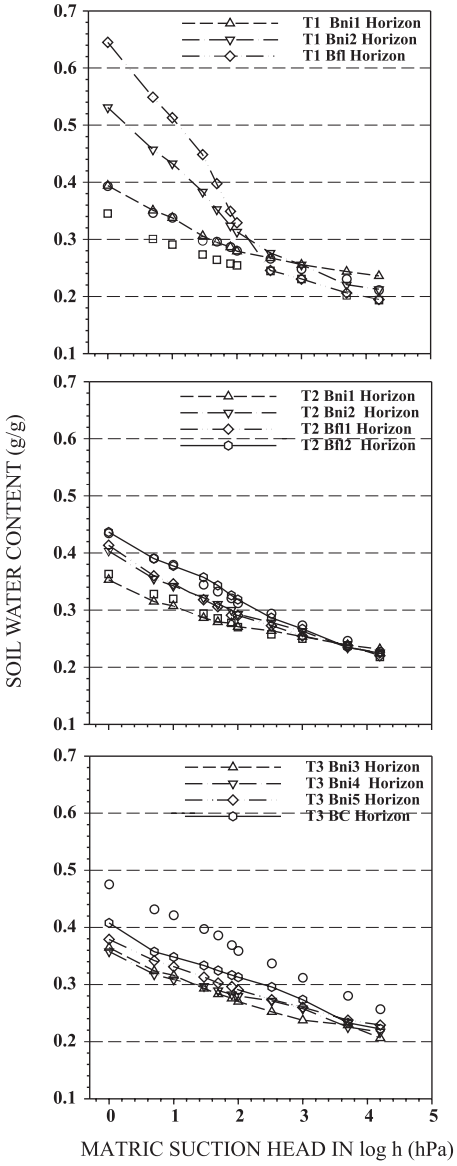

Figure 5. Soil water characteristic curves of each profile (T1, T2 and T3).

between these horizons (as described above). Although the differences in slope gradient are quite pronounced, the transition between the Bfl horizon and the Bni1 horizon occurs gradually and in the range of gravimetric water content that correspond to the matric potentials (h) of 1 to 200 hPa (log h = 0 to 2.3). The differences in the slope gradient in T2 practically disappear from the Bni to the Bfl horizons. A marked difference can still be observed between Bni1 and Bfl2 horizons, while the gradients of the Bni2 and Bfl1 horizons were intermediate, resulting in transitional horizons. No differences were observed in the slope gradient between the soil water characteristics of the horizons in T3. A slight increment in the slope gradient of the transition horizon to the saprolite can be attributed to the incipient microaggregation observed in this horizon.

The changes in the behavior of the soil water characteristic curves within the different B horizons can be seen in figure 6. In all cases (Bni1, Bni2, Bni3, Bni4, BC, and Bfl), a decrease in the slope gradient of the curves, within the different horizons, occurs from the summit to the shoulder position showing that changes in aggregation, pore size, pore distribution, and pore morphology do not only occur vertically but also laterally within horizons with similar field morphological properties.

The vertical and lateral evolution of the soil water characteristic curves of this toposequence showed that the changes occur mainly in the part of the curve related to the structural porosity. This phenomenon evidences a gradual compaction process from the Bfl to the Bni horizons and also within the different B horizons as they evolve from the summit to the shoulder positions.

Seasonal variations of the total potential head

The seasonal variations of the soil water total potential head of the four tensiometric stations (TS) on the toposequence (Figure 1) are shown in figures 7 and 8.

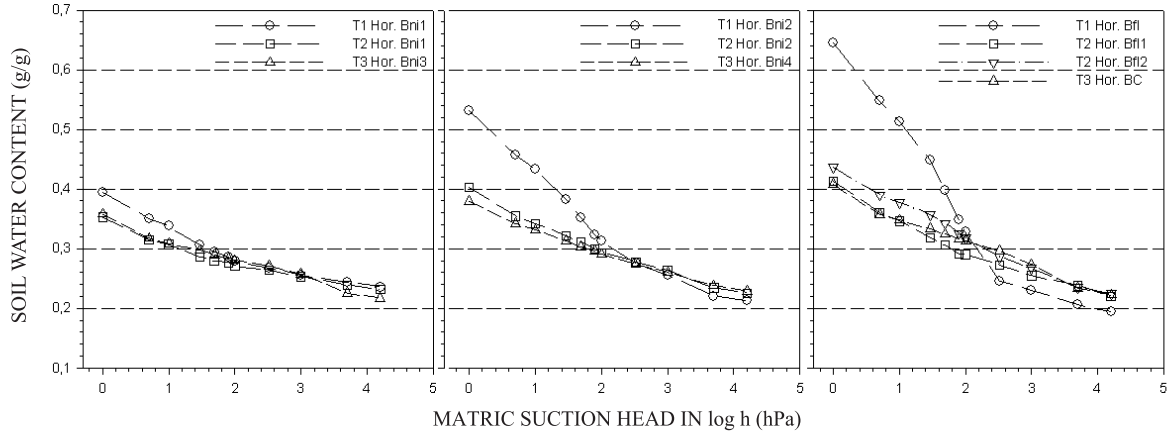

Figure 6. Comparison between the soil water characteristic curves of the Bni and Bfl horizons situated in different positions on the toposequence.

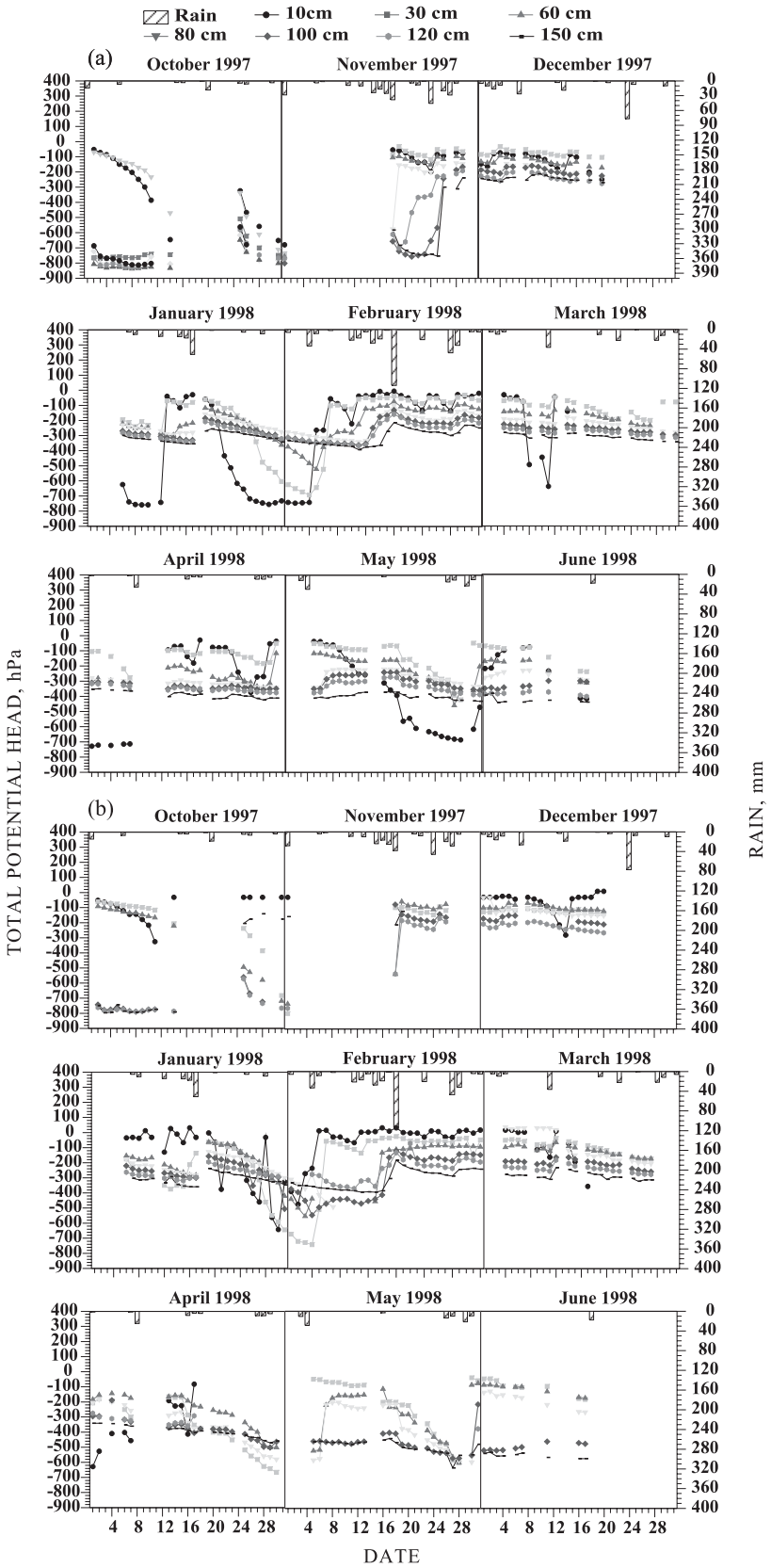

Figure 7. Daily variations of the total water potential head in tensiometric station 1 (TS1) situated in the summit segment (a), and in tensiometric station 2 (TS2) situated at the transition between the summit and upper shoulder segments (b). Blank spaces in the graphs correspond to periods where no measurements could be made or to problems with the functioning of the tensiometers.

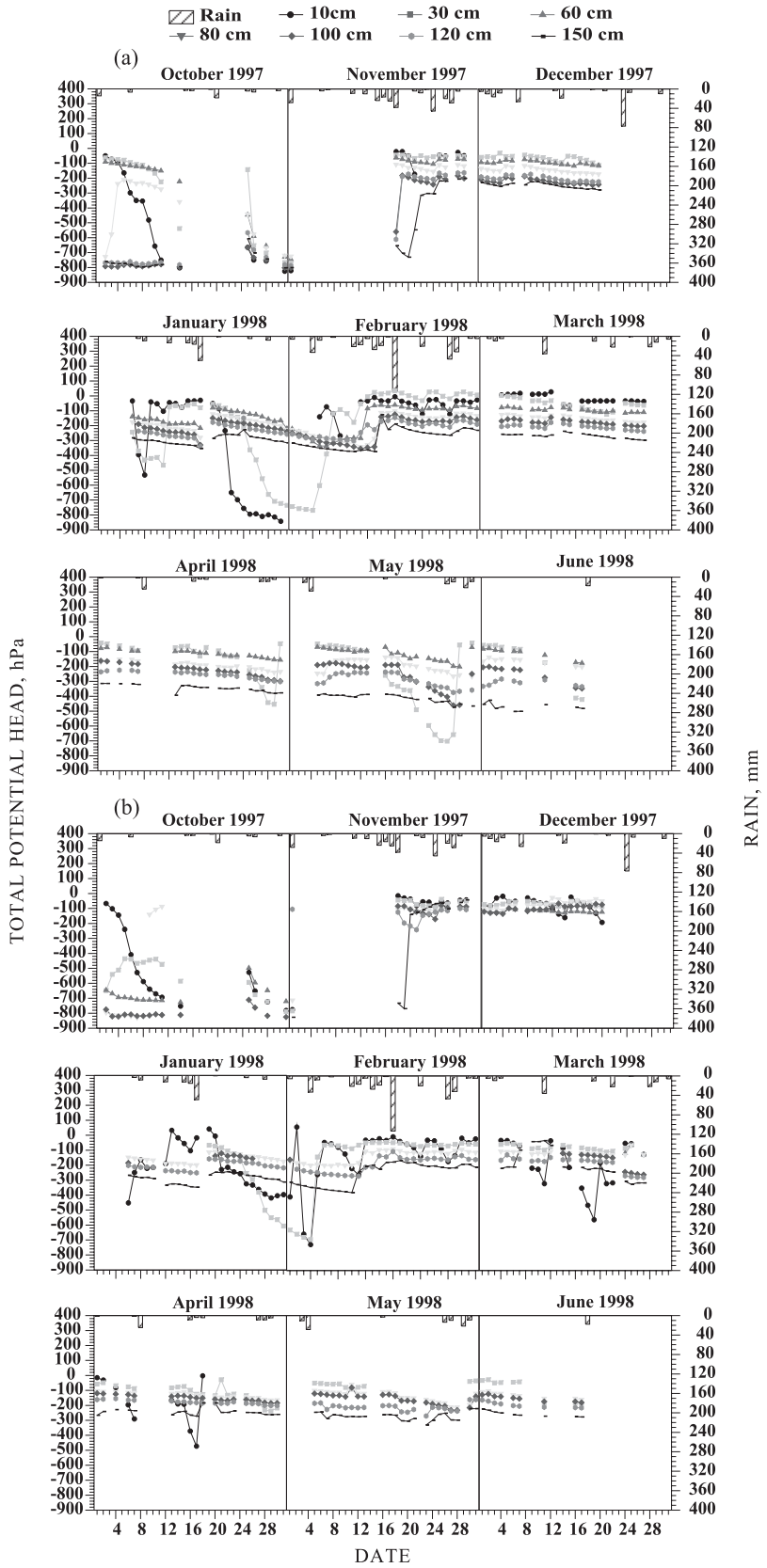

Figure 8. Daily variations of the total water potential head in tensiometric station 3 (TS3) situated in upper shoulder segment (a), and in tensiometric station 4 (TS4) situated in lower shoulder segment (b). Blank spaces in the graphs correspond to periods where no measurements could be made or to problems with the functioning of the tensiometers.

The behavior to the seasonal variations of the total water potential head was similar in all four TS. Two distinct periods were identified, one represented by low water potential heads (between -600 and -800 hPa) in the dry winter months (July to September, not shown) and the other by fairly high water potential heads (between 0 and -300 hPa) in the wet summer months (November to March). The end of the dry season and beginning of the wet season (September and October) is marked by sporadic and concentrated rainfalls with medium to low intensities that lead to a rapid wetting of the soil surface horizons (down to approximately 0.6 m). In November, in the full rainy season, the subsurface horizons (below 0.6 m) behave similarly to surface horizons and the total water potential heads increase rapidly to values that remain practically constant in the whole summer or wet season. On the other hand, the tensiometers showed that the soil drying process occurs very slowly and gradually with practically no differences between the horizons between April and June, with exception of the surface horizon (0.1 m). These measurements show that the period in which the soil is truly dry in the year is very short whereas the period in which the soil is moist or subjected to moisture fluctuations is quite long.

The data presented in figures 7 and 8 show that the water movement in the soil toposequence is eminently vertical, from the A horizons (10cm) down to the Bfl or deeper (150 cm) horizons. No evidences of lateral water movement or seasonally perched water tables were found in this transect.

This preferential vertical movement of water in these soils was confirmed by monitoring the total water potential head in some rainstorm events. Figure 9 shows the evolution of the total water head potential in a rainstorm that occurred in the morning of 16/2/1998.

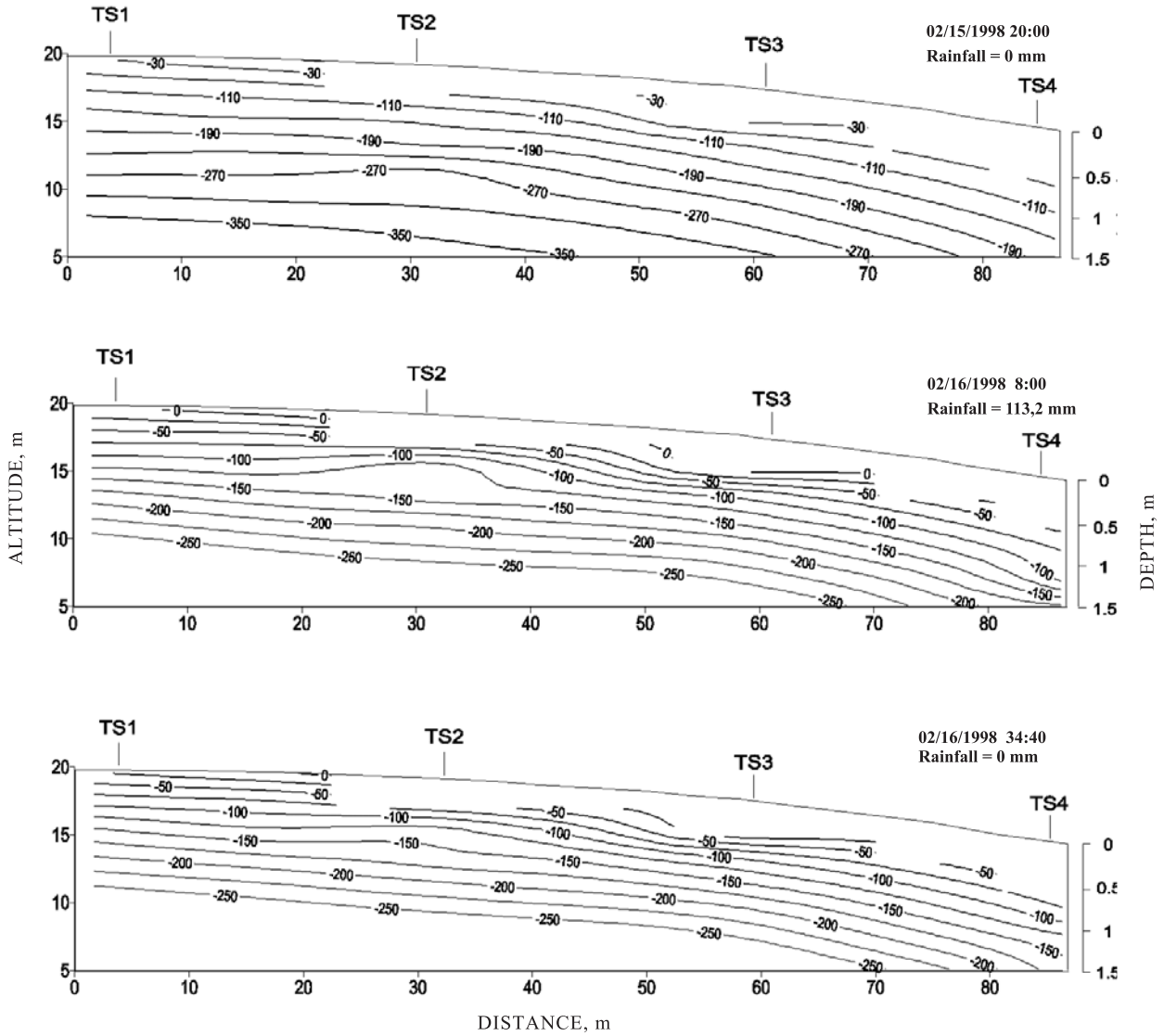

Figure 9. Total water potential head variations during a rainstorm in the morning of 16/2/1998. Isolines in hPa were made using geostatistical gridding methods (Krigging).

During this rain event saturation was attained in A and BA horizons (tensiometers at 0.1 and 0.3 m, respectively) affecting runoff formation, but even in this situation water redistribution within the soil was shown to have a vertical direction from the surface to the deeper horizons.

DISCUSSION

The distribution of the soil horizons and their soil structure characteristics evidenced a vertical and lateral structural transformation. This transformation occurs between microaggregate structured horizons (ferralic horizon) and polyhedral structured horizons (nitic horizon). The lateral transition can be characterized as very progressive and the vertical transition between the different horizons is diffuse. Changes in the pore morphology, pore distribution, water retention characteristics and soil aggregation occur as a consequence of this process.

To understand the structural evolution, four stages similar to the ones described by Miklós (1992), were suggested. The first stage corresponds to the microaggregate structure, characterized by packing voids and an enaulic C/F related distribution. The second stage is represented by a transition where a porphyro-enaulic C/F related distribution dominates. It is characterized by the appearance of polyconcave vughs, that result from the coalescence of oval and polyhedral microaggregates, and a reduction of the pore space. The third stage represents a porphyric C/F related distribution and a drastic reduction of the pore space, where vughs and polyconcave vughs dominate. The fourth stage corresponds to the presence of polyhedral aggregates with a porphyric C/F related distribution and porosity formed by planar voids and polyconcave vughs within the aggregates.

Three processes were identified as responsible for the formation of this structural evolution: microaggregate coalescence, clay illuviation and fissuration. The results presented by Fedoroff & Eswaran (1985), who studied soils with argillic and oxic horizons, showed a similar sequence of processes; the formation of the argillic horizon would begin with the compaction of the microaggregates of the oxic horizon followed by clay deposition covering the aggregates and filling the packing voids.

The coalescence of the microaggregates would occur by an approximation and welding of the microaggregates due to soil wetting and drying processes and compression forces provoked by biological activity (root growth and/or macro and mesofauna activity). The existence of an energetically contrasting environment due to wetting and drying cycles would induce the appearance of very high tension forces in the soil matrix that would correspond to water tensions varying between 0 and -600kPa in a year, according to Pedro (1987). These would approximate and coalesce the microaggregates. This situation would occur in a dryer climate, probably ustic or semiarid (Miklós, 1992), that would form an energetically contrasting environment due to the existence of very different climatic seasons characterized by short wet seasons (usually isolated torrential rains) and long dry seasons (Miklós, 1992). The approximation and contact between the microaggregates would occur by the expansion of these aggregates in the short wetting phase (low tension forces). A posterior transition to a drying phase (high tension forces) would lead to the contraction of the soil matrix and the welding of the contact regions between the microaggregates. The stability of the coalesced microaggregates would depend on the size of the contact area and long dry seasons that lead to high tension forces in the soil.

In disagreement with this hypothesis Moniz & Buol (1982), Moniz (1996) and Vidal-Torrado et al (1999) explained the formation of the nitic and argillic horizons from ferralic horizons by compaction processes due to actual alternating saturation and dessication cycles formed by the subsoil lateral-water flow along the slope. The soil water dynamics data presented above showed that the direction of water flow in these soils was vertical; no subsurface lateral water flow was evidenced. The data also showed that the variation of total water potential head of these soils per year varied between 0 and –80kPa, which is very distant from the energy contrasts suggested by Pedro (1987) for microaggregate coalescence, and that the dry periods were too short to stabilize the coalesced microaggregates. Consequently, supporting the hypothesis presented above, the water tensions determined by actual soil water dynamics of this toposequence would not be sufficient to form the compacted horizon and the absence of lateral-water flow invalidates the conclusions presented by Moniz & Buol (1982) and Vidal-Torrado et al (1999) for the toposequence studied in this paper.

Biological activity is high in all toposequence as found in the morphological and micromorphological descriptions. The pressure exerted by the burrowing action of the soil macro and mesofauna and root penetration through the soil matrix leads to the formation of channels and vughs with densed walls. The formation of biological channels and vughs in microaggregated horizons leads to the approximation and coalescence of the microaggregates around pore walls. The high incidence of biological activity in these soils show the importance of this process in the coalescence of microaggregates and the compaction of the ferralic horizons.

Clay illuviaton features were found in all B nitic horizons filling the polyconcave vughs, packing and planar voids. Although this process is secondary in relation to microaggregate coalescence, it also participates in the compaction process as a result of

the reduction of the pore space by clogging voids. This process has been widely discussed by Lepsch et al. (1977), Fedoroff & Eswaran (1985), Creutzberg & Sombroek (1987), Moniz (1996), Vidal-Torrado et al. (1999), and Cooper & Vidal-Torrado (2000).

The formation of polyhedral macroaggregates (blocky structure) and of interaggregate planar voids, characteristic of the fourth stage, occurs as a result of the fissuration process of the porphyric and porphyro-enaulic C/F related distribution. An intensification of this process would also be responsible for the formation of polyhedral microaggregates observed at the transitions between the compacted nitic horizons and the ferralic horizons. Frequent contraction and expansion processes due to alternate drying and wetting cycles would form the planar voids. This process would result from seasonal climatic alternations that occur in humid climates where the energetic contrasts are smaller leading to the retraction of the material and consequent fissuration (Pedro, 1987; Miklós, 1992). As the soil water dynamics data presented above show, in this toposequence there would not be enough energy to approximate and coalesce the microaggregates, consequently resulting in a fragmentation or fissuration process of the compact and transition horizons.

CONCLUSIONS

1. The soil morphology and water processes of the lateral and vertical transition between microaggregate and polyhedral aggregate horizons showed that the structural transformation of these horizons occurs by a compaction process due to hydro-physical and mechanical restrictions.

2. The coalescence process would occur by alternating wetting and drying cycles. The initial contact between the microaggregates would occur in short wetting phases and the welding of the coalesced microaggregates in intense, long drying phases. High energetic contrasts that occur in drier climates than present (ustic or semi-arid) would be necessary to stabilize the coalesced microaggregates. Further experimental studies are needed to demonstrate this conclusion.

3. Other compacting processes such as the mechanical action of soil biological activity and pore clogging by clay illuviation were identified. The extent of these processes indicates their importance for the structural transformation observed in this toposequence.

4. The formation of polyhedral aggregates and polyhedral microaggregates is an ongoing process and results from fissuration processes which in turn result from soil contraction and expansion in the present humid climate (low energetic contrast between wet and dry seasons).

ACKNOWLEDGEMENTS

The authors wish to thank Janine Berrier for her advice with the scanning electron microscopy studies, Yanninck Benard for preparing the soil thin sections, the Soil and Plant Nutrition Department of the ESALQ/USP and the Unité Mixte de Recherche Sol-Agronomie Spatialisation of the INRA (Rennes-France) for the use of the laboratories and facilities for this research, and FAPESP (Fundação de Amparo à Pesquisa do Estado de São Paulo) and CAPES (Coordenação de Aperfeiçoamento de Pessoal de Nível Superior) for the financial support.

LITERATURE CITED

BOULET, R.; CHAUVEL, A.; HUMBEL, F.X. & LUCAS, Y. Analyse structurale et cartographie en pédologie. I Prise en compte de l´organisation bidimensionelle de la couverture pédologique: Les études de toposéquences et leurs principaux apports à la connaissance des sols. Cah. ORSTOM, Sér. Pedol., 19:309-320, 1982.

BREWER, R. Fabric and mineral analysis of soils. New York, Robert E. Krieger Publishing Company. 1976. 482p.

BULLOCK, P. & THOMPSON, M.L. Micromorphology of Alfisols. In: DOUGLAS L.A. & THOMPSON, M.L., eds. SOIL MICROMORPHOLOGY AND SOIL CLASSIFICATION, Anaheim, 1985. Proceedings... Anaheim, 1985. p.17-47.

BULLOCK, P.; FEDOROFF, N.; JONGERIUS, A.; STOOPS, G.; TURSINA, T. & BABEL, U. Handbook for soil thin section description. Wolverhampton, Waine Research Publication, 1985. 152p.

COOPER, M. & VIDAL-TORRADO, P. Gênese de ferri-argilãs em horizontes B texturais de uma sequência de solos sobre diabásio em Piracicaba (SP). Sci. Agríc., 57:745-750, 2000.

COOPER, M. & VIDAL-TORRADO, P. Caracterização morfológica, micromorfológica e físico-hídrica de solos com horizonte B nítico. R. Bras. Ci. Solo, 29:581-595, 2005.

COOPER, M.; VIDAL-TORRADO, P. & LEPSCH, I.F. Stratigraphical discontinuities, tropical landscape evolution and soil distribution relationships in a case study in SE-Brazil. R. Bras. Ci. Solo, 26:673-683, 2002.

CREUTZBERG, D. & SOMBROEK, W.G. Micromorphological characteristics of Nitosols. In: RÉUNION INTERNATIONALE DE MICROMORPHOLOGIE DES SOLS, 7., Paris, 1987. Actes... Paris, 1987. p.151-155.

FEDOROFF, N. & ESWARAN, H. Micromorphology of ultisols. In: DOUGLAS L.A. & THOMPSON, M.L., eds. SOIL MICROMORPHOLOGY AND SOIL CLASSIFICATION, Anaheim, 1985. Proceedings... Anaheim, 1985. p.145-164.

ISSS-ISRIC-FAO. World reference base for soil resources. Rome, 1998. (World Resources Report, 84)

LEMOS, R.C. & SANTOS, R.D. Manual de descrição e coleta de solos no campo. 3.ed. Campinas, Sociedade Brasileira de Ciência do Solo, 1996. 84p.

LEPSCH, I.F. & BUOL, S.W. Investigations in an Oxisol-Ultisol toposequence in São Paulo State, Brazil. Soil Sci. Soc. Am. Proc., 38:491-496, 1975.

LEPSCH, I.F., BUOL, S.W. & DANIELS, R.B. Soil landscape relationships in the occidental plateau of São Paulo, Brazil: I. Geomorphic surfaces and soil mapping units. Soil Sci. Soc. Am. J., 41:104-109, 1977.

MIKLÓS, A.A.W. Biodynamique d'une coverture pédologique dans la région de Botucatú, Brésil. Paris, Université de Paris VI, 1992. 2v. 438p. (Tese de Doutorado)

MONIZ, A.C. Evolução de conceitos no estudo da gênese de solos. R. Bras. Ci. Solo, 20:349-362, 1996.

MONIZ, A.C. & BUOL, S.W. Formation of an Oxisol-Ultisol transition in São Paulo, Brazil: I - Double-water flow model of soil development. Soil Sci. Soc. Am. J., 46:1228-1233, 1982.

MORAN, C.J.; KOPPI, A.J.; MURPHY, B.W. & MCBRATNEY A.B. Comparison of the macropore structure of a sandy loam surface soil horizon subjected to two tillage treatments. Soil Use Manag., 4:96-102, 1988.

MURPHY, C.P. Thin section preparation of soils and sediments. Berkhamsted, A B Academic Publishers, 1986.149p.

PEDRO, G. Géochimie, mineralogie et organisation des sols. Aspects coordonnés des problèmes pédogénétiques. Cah. Orstom, Série Pédol., 23:169-186, 1987.

VIDAL-TORRADO, P. & LEPSCH, I.F. Morfogênese dos solos de uma topossequência com transição B Latossólico x B textural sobre migmatitos em Mococa (SP). R. Bras. Ci. Solo, 17:109-119, 1993.

VIDAL-TORRADO, P.; LEPSCH, I.F.; CASTRO, S.S. & COOPER, M. Pedogênese em uma sequência Latossolo-Podzólico na borda de um platô na Depressão Periférica Paulista. R. Bras. Ci. Solo, 23:909-921, 1999.